Hypothesis

A 3D model of the voltage-dependent anion channel (VDAC)

Rita Casadio[a,b], Irene Jacoboni[a], Angela Messina[c], Vito De Pinto[c,*]

[a]*Laboratory of Biocomputing, Centro Interdipartimentale per le Ricerche Biotecnologiche (CIRB), Bologna, Italy*
[b]*Laboratory of Biophysics, Department of Biology, University of Bologna, Bologna, Italy*
[c]*Laboratory of Biochemistry and Molecular Biology, Department of Chemical Sciences, University of Catania, Viale A. Doria 6, 95125 Catania, Italy*

Abstract Eukaryotic porins are a group of membrane proteins whose best known role is to form an aqueous pore channel in the mitochondrial outer membrane. As opposed to the bacterial porins (a large family of protein whose 3D structure has been determined by X-ray diffraction), the structure of eukaryotic porins (also termed VDACs, voltage-dependent anion-selective channels) is still a matter of debate. We analysed the secondary structure of VDAC from the yeast *Saccharomyces cerevisiae*, the fungus *Neurospora crassa* and the mouse with different types of neural network-based predictors. The predictors were able to discriminate membrane β-strands, globular α-helices and membrane α-helices and localised, in all three VDAC sequences, 16 β-strands along the chain. For all three sequences the N-terminal region showed a high propensity to form a globular α-helix. The 16 β-strand VDAC motif was thus aligned to a bacterial porin-derived template containing a similar 16 β-strand motif. The alignment of the VDAC sequence with the bacterial porin sequence was used to compute a set of 3D coordinates, which constitutes the first 3D prediction of a eukaryotic porin. All the predicted structures assume a β-barrel structure composed of 16 β-strands with the N-terminus outside the membrane. Loops are shorter in this side of the membrane than in the other, where two long loops are protruding. The shape of the pore varies between almost circular for *Neurospora* and mouse and slightly oval for yeast. Average values between 3 and 2.5 nm at the C-carbon backbone are found for the diameter of the channels. In this model VDAC shows large portions of the structure exposed on both sides of the membrane. The architecture we determine allows speculation about the mechanism of possible interactions between VDAC and other proteins on both sides of the mitochondrial outer membrane. The computed 3D model is consistent with most of the experimental results so far reported. © 2002 Published by Elsevier Science B.V. on behalf of the Federation of European Biochemical Societies.

Key words: Porin; Voltage-dependent anion-selective channel; Neural network; Prediction of membrane porin; Pattern recognition; Membrane β-strand

1. Introduction

Eukaryotic porins are a group of membrane proteins whose best known role is to form an aqueous pore channel in the mitochondrial outer membrane [1–3]. As opposed to bacterial

porins (a large family of proteins) and other outer membrane receptors, whose 3D structure has been determined by X-ray diffraction (for reviews see [4,5]; for the main determined structures see [6–11]), the structure of eukaryotic porins (also termed VDACs, voltage-dependent anion-selective channels) is not known at a useful resolution. This is a lack in our knowledge of the molecular process associated with the physiological role of the protein. VDAC is an important node in the cellular cross-talk between the mitochondrion and the rest of the cell. Its role as the mitochondrial receptor of hexokinase was elucidated several years ago [12,13]. Recently it was claimed to be involved in multisubunit complexes like the permeability transition pore [14], the contact sites [15], and others [16]. A crucial role for this channel is also presumed in the early steps of the mitochondrially dependent apoptotic cascade and, in general, more features than the simple channel activity are suspected in a cellular context (for a review see [17]).

VDAC has been crystallised only at very low resolution (about 0.8 nm [18]). Additional structural information about VDAC pore and its domains was obtained by electron microscopy of negatively stained and frozen-hydrated 2D crystals of fungal VDAC [19,20]. The apparent impossibility to get VDAC crystals useful for X-ray diffraction analysis caused the flourishing of theoretical models of transmembrane arrangements of the protein. They were based on predictions of the secondary structure and were usually probed by experimental approaches. Unfortunately these models showed a large pattern of differences [21–25].

In this hypothesis paper we suggest a new model of VDAC transmembrane arrangement. It is based on a threading procedure, which starts with a new neural network-based predictor suited to locate β-strands along a given protein sequence [26]. The predictor is trained to recognise the topography of the protein β-strands by training on a non-redundant set of bacterial β-barrel membrane proteins known at atomic resolution. The output of this prediction is then used to align VDAC to a template bacterial porin.

The result is a low-resolution 3D model of a VDAC channel in the open conformation, useful to design new experiments in order to highlight the putative roles of eukaryotic porins.

2. Building the model

The sequences of the VDAC from three different species were considered for modelling (VDAC from *Neurospora cras-*

*Corresponding author. Fax: (39)-95-337036.
E-mail address:* vdpbiofa@mbox.unict.it (V. De Pinto).

sa, yeast *Saccharomyces cerevisiae* and the mouse isoform 1 or MVDAC1). The choice of these three species was made both to get the most general overview of VDAC characteristics, and also to compare our models with the experimental characterisation described in the literature for these species. The three protein sequences selected share different extents of identity, although they are associated with the same function. Indeed, pair-wise sequence alignment between *Neurospora* and yeast VDACs gives the highest sequence identity (equal to 40%) whereas sequence homology between *Neurospora* and mouse VDAC and between yeast and mouse VDAC is only 29 and 25%, respectively.

In order to predict the structure of VDACs we used the newly implemented neural network predictor specifically suited to localise the position of β-strands of outer membrane proteins [26]. The result of this analysis is the localisation of 16 β-strands along the sequence (shown in Fig. 1). Since it has been recognised with different approaches [21,22,27] that one of the major distinctions between VDAC and bacterial porins is the presence of an α-helix at the N-terminus of the mitochondrial channel, we used two other types of neural networks to investigate the length and the position of this helix with respect to the membrane. The first predictor was specific for globular α-helices [28], the second for membrane α-helices [29]. Neural network profiles revealed the presence of an N-terminal α-helix from residue 9 to residue 18, and that this helix is not embedded in the membrane (the neural net-

work specific for membrane α-helices predicted no significant signal in any part of the sequence).

Modelling of VDACs was then performed considering the results described above and excluding the N-terminal portion of the sequence containing the globular α-helix. This N-terminal part of the sequence was subsequently added to the final model with WHATIF [30]. The modelling procedure is essentially that of building by homology with the exception that alignment of the target to the templates is based on secondary structure (Fig. 1). The modelling procedure of MODELLER [31] allows selection of more than one template: three bacterial porins were selected from the PDB database (2OMF, 1PRN and 2POR), each of them sharing the same structure but very low sequence identity (below 30%). Positioning had as a reference the 16 β-strands predicted in each sequence, which were manually centred and located below the counterparts in the porin crystallised sequences (one of the alignments is given in Fig. 1). Gaps were confined to the loop regions: this was necessary since loops in the bacterial porins are longer than those in the VDACs. The manual procedure adopted can give different alignments. For each sequence, each alignment was modelled and the model that had the best PROCHECK [32] score (minimum percentage of residues in disallowed conformation) was adopted as the final result.

The evaluation results indicate that the *Neurospora* and yeast models are characterised by a percentage of residues in allowed regions comparable with that of a crystal with a resolution < 0.2 nm (data not shown). This value becomes 0.25 nm for the mouse VDAC. For each species there is only one residue in a disallowed region outside a loop at the end of a β-strand. This small percentage (0.3%) can be also found in protein crystals, as for example in 1PRN. The rest of the residues in disallowed conformations (5%) are confined in the loops whose coordinates strongly depend on the amino acid composition of the specific protein considered. The 3D model of *Neurospora* VDAC is shown in Fig. 2. The models for *Neurospora*, yeast and mouse (isoform 1 or MVDAC1) porins are very similar. All the proteins assume a β-barrel structure composed of 16 β-strands with the α-helix at the N-terminus outside the membrane. The C-terminus is positioned at the same side of the α-helix, with the very last residues possibly protruding outside the membrane (see arrow). The α-helix is a sketch to indicate the position of this structure relative to the membrane and its actual orientation could be different from the one reported. It must be noticed that not all the about 20 N-terminal residues in the sequence have a high probability to form an α-helix. Residues 1–8 are predicted to be in a more random conformation, while α-helix is predicted between 9 and 19 (data not shown). The reduction of residues involved in the α-helix improves its amphiphilicity since Pro4 biased the hydrophilic side as can be observed in its helical wheel projection [27]. The features described below (dimensions, charge position and loop length) are similar for all three models. On the opposite side of the N- and C-termini, two long loops protrude outside the membrane. In one of these loops a small fragment of an α-helix is visible. These small fragments can be found in bacterial porins and also occur in VDAC, given the model building procedure. On the other side of the membrane, loops are short. Bacterial porins also have long loops on one side and short loops on the other side of the membrane. The model, in fact, resembles the template, but it is not identical. For example, the loop that


```
2omf_.seq/ AEIYNKDGNK  VDLYGKAVGL  HYFSKGNGEN  SYGGNGDMTY  ARLGFKGETQ
2omf_.str/ CCCCCCCCEE  EEEEEEEEEE  EEECCCCCCC  CCCCCCCCCE  EEEEEEEEEE
protx.str/ *******CCC  CCCCEEEEEE  EEEC******  ********CE  EEEEEEEECC
protx.seq/ *******KGY  NFGLWKLDLK  TKTS******  ********SG  IEFNTAGHSN

2omf_.seq/ I*NSDLTGYG  QWEYNFQGNN  SEGADAQTGN  KTRLAFAGLK  YADVGSFDYG
2omf_.str/ C*CCCEEEEE  EEEEEEECCC  CCCCCCCCCC  EEEEEEEEEC  CCCCCEEEEE
protx.str/ CCCCCEEEEE  EEEEEEC***  **********  EEEEEEEEEC  CCCCCEEEEE
protx.seq/ QESGKVFGSL  ETKYKVK***  **********  DYGLTLTEKW  NTDNTLFTEV

2omf_.seq/ RNYGVVYDAL  GYTDMLPEFG  GDTAYSDDFF  VGRVGGVATY  RNSNFFGLVD
2omf_.str/ ECCCCCCCCC  CCCCCCCCCC  CCCCCCCCCC  CCCCCCEEEE  EECCCCCCCC
protx.str/ EEEECC****  **********  **********  **CCEEEEEE  EEECCCCCCC
protx.seq/ AVQDQL****  **********  **********  **LEGLKLSL  EGNFAPQSGN

2omf_.seq/ GLNFAVQYLG  KNER******  *******D   TARRSNGDGV  GGSISYEYE*
2omf_.str/ CEEEEEEEEC  CCCC******  *******C   CCCCCCCCEE  EEEEEEEEC*
protx.str/ EEEEEEEEE   EEEECCCCCC  CCCCCCCCEE  EEEEEEEEE   CCCCCEEECC
protx.seq/ KNGKFKVAYG  HENVKADSDV  NIDLKGPLIN  ASAVLGYQGW  LAGYQTAFDT

2omf_.seq/ **GFGIVGAY  GAADRTNLQE  AQPLGNGKKA  EQWATGLKYD  ANNIYLAANY
2omf_.str/ **CEEEEEEE  EEEECCCCCC  CCCCCCCCEE  EEEEEEEEEE  ECCEEEEEEE
protx.str/ CCEEEEEEEE  EEEEEEEEEE  CCCCCCCCEE  EEEEEEEEE   EEEEEEEEEE
protx.seq/ QQSKLTTNNF  ALGYTTKDFV  LHTAVNDGQE  FSGSIFQRTS  DKLDVGVQLS

2omf_.seq/ GETRNATPIT  NKFTNTSGFA  NKTQDVLLVA  QYQFDFGLRP  SIAYTKSKAR
2omf_.str/ EEEECCCCCC  CCCCCCCCCC  CEEEEEEEEE  EEECCCCCEE  EEEEEEEEEE
protx.str/ EEECC*****  **********  *CCCEEEEEE  EEECCCCCEE  EEEEEEC***
protx.seq/ WASGT*****  **********  *SNTKFAIGA  KYQLDDDARV  RAKVNNA***

2omf_.seq/ DVEGIGDVDL  VNYFEVGATY  YFNKNMSTYV  DYIINQIDSD  NKLGVGSDDT
2omf_.str/ CCCCCCCEE   EEEEEEEEEE  EECCCCEEEE  EEEEECCC**  CCCCCCCCCC
protx.str/ *******E   EEEEEEEEE   EC***EEEE   EEEECCC**   *****CCCCE
protx.seq/ *******S   QVGLGYQQKL  RT***GVTLT  LSTLVDGK**  *****NFNAG

2omf_.seq/ VAVGIVYQF*  **
2omf_.str/ EEEEEEEEE*  **
protx.str/ EEEEEEEEE   EC*
protx.seq/ GHKIGVGLEL  EA*
```

Fig. 1. Threading of the target to the template. The β-strands predicted by the neural network along the target protein sequence (protx.seq, corresponding to the protein sequence of the *N. crassa* VDAC) are aligned with the secondary structure of a 16 β-strand template (the bacterial porin 2omf (2omf.str)). For the sake of clarity both the target and template protein sequences are also shown. Prediction is performed as previously described [26] and alignment of secondary structures is performed conserving β-strand positions and constraining gaps to the loop regions.

Loop side

Fig. 2. Different views of the predicted 3D structure of *N. crassa* VDAC. The model consists of a β-barrel containing 16 β-strands and a globular α-helix sketched using WHATIF. We added the amino acids at the terminal region of the β-barrel in a defined conformation according to secondary structure prediction. The shape and orientation of the N-terminal end and of the major loops was by no means a predicted one, but they have to be considered just a cartoon. 3D models for yeast and mouse VDAC are very similar.

in the bacterial porins occludes the channel (loop 5) is much shorter in the model (due to the alignment of secondary structures) and cannot occlude the channel. On the other hand, for example, loop 7 is much longer than the corresponding loop in the bacterial porins and may occlude the channel. It has to be noticed, indeed, that the longer loops are not frozen in the indicated position, and may probably occlude the channel in some circumstances. The shape of the pore varies slightly along the sequences: it is circular for *Neurospora* and mouse and slightly oval for yeast (see Fig. 2). Average values of 3 and 2.5 nm are found for the external and internal diameters of the channel, respectively. All the charged residues in the barrel are oriented with the charge inside the β-barrel, towards the aqueous channel; charges in loops are randomly oriented.

3. Is it correct to compare eukaryotic VDACs to prokaryotic porins?

Gram-negative bacteria and mitochondria share in many respects a similar organisation [33]. Two membranes surround them both and the presence of a pore-forming protein with a similar sieving function in the outer membrane of mitochondria and bacteria is suggestive of a relationship between them.

On the other hand, very little sequence similarity between bacterial and eukaryotic porins (VDACs) exists. Even comparison between bacterial porin groups revealed an average identity of $13 \pm 1\%$ [34]. Porin proteins are indeed a clear case of secondary structure conservation during evolution. The secondary structure typical of bacterial porins is the amphipathic β-strand: they are assembled in a transmembrane β-barrel. They were also detected in eukaryotic VDACs [21–24] based on computer programs able to reveal the regular alternation of polar and non-polar residues in amino acid sequences [35]. An improvement in the structural information available by a computational approach was the Bayesian statistical algo-

rithm called the Gibbs sampler [36]. Its application to sequences of bacterial outer membrane protein found a short (11–13 residue) repetitive sequence pattern [37]. This motif corresponded to β-strands in bacterial porins of known structure. The only match of this motif to eukaryotic proteins detected mitochondrial porin and Tom40, another mitochondrial outer membrane protein [38]. Attenuated total reflection Fourier transform infrared spectroscopy recently confirmed that both prokaryotic and eukaryotic proteins contain a similar 50–53% of the β-barrel structure [39].

When we look at the differences between bacterial porins and VDACs we should suppose an adaptation to the intracellular localisation with respect to the harmful environment that the bacterial outer membrane has to deal with. The screening properties owned by bacterial porins (due to the large loops folded inside the pore) and the structural robustness associated with the alkali- and heat-resistant trimeric organisation were no longer essential for the mitochondrial protein. With a similar number of amino acids, single subunits in the eukaryotic counterpart could form a pore adapted to a less selective traffic across the membrane. The diameter at the Cα backbone is similar between bacterial porins and our model of eukaryotic VDAC. But the exclusion limits are different [4]. This is not surprising when we assume the lack of several large folded loops in the mitochondrial protein. The larger water-accessible size of the eukaryotic pore was deduced by single channel reconstitution experiments [1,3,4] and by projection images of VDAC arrays obtained by electron microscopy and correlation averaging [13,40]. These data indicated a width of 5–6 nm and a mean diameter of the VDAC pore at the C-α backbone of 3.6–3.8 nm.

The main novelty in VDAC is the reported presence of an amphipathic α-helix at the N-terminus. We predict this secondary structure limited to residues 9–18, confirming early observations of the circular dichroism spectra of VDAC's N-terminal peptide, which showed a maximum α-helix con-

Fig. 3. Comparison of current topological models of eukaryotic VDACs with the model presented in this work. The models were depicted as 2D projections, with ribbons indicating the β-strands and a cylinder indicating the α-helix. A: The 12 β-strand/one α-helix model designed for yeast [45]. Boxed residues were considered essential for the pore ionic selectivity. B: A view of our yeast model, where the same residues considered essential for the pore ionic selectivity were evidenced. C: The 13 β-strand/one α-helix model designed for *N. crassa* [47]. Type 1 residues (mapped as exposed residues) are circled, type 2 residues (considered of relevance for the voltage dependence property) are boxed. D: A view of our *N. crassa* model, where the position of type 1 and type 2 residues is shown with the same formalism as in C.

tent of 40–50% [40]. The amphiphilicity of this amino acid stretch in any case suggests some interaction with an hydrophobic milieu, which the core of the phospholipid bilayer is. This α-helix, located on one side of the membrane, might be of relevance in functions attributed to VDAC, which contrast to its rigid β-barrel arrangement, in particular in the voltage dependence. This is the pore partial closure in response to modest transmembrane potentials of both polarities (voltage-gating [41,42]). Voltage-gating in eukaryotic VDAC is in the low voltage range of about 30–40 mV as compared to the voltage-gating of bacterial porins, which needs voltages above 100 mV [43]. It is suggestive to consider that the addition of the N-terminal α-helix to the eukaryotic pore during evolution might have something to do with the addition of this property to VDAC. Unfortunately it is not clear at a molecular level how the voltage shift is sensed by the protein

and what changes in the structure are triggered by such a voltage dependence.

The N-terminal α-helix, located on one side of the membrane, together with the relatively large hydrophilic loops, located on the other side, might also mediate the reported interactions of VDAC with other proteins like modulators [44], glycolytic enzymes [12,13] or components of multisubunit complexes (contact sites, import complex, permeability transition pore) [14–17].

4. Fitting of the model to experimental results

Results obtained with various approaches have been used in the last 10 years to suggest different models of transmembrane arrangement of eukaryotic porins. We can summarise these experiments in two main groups: site-directed mutagenesis
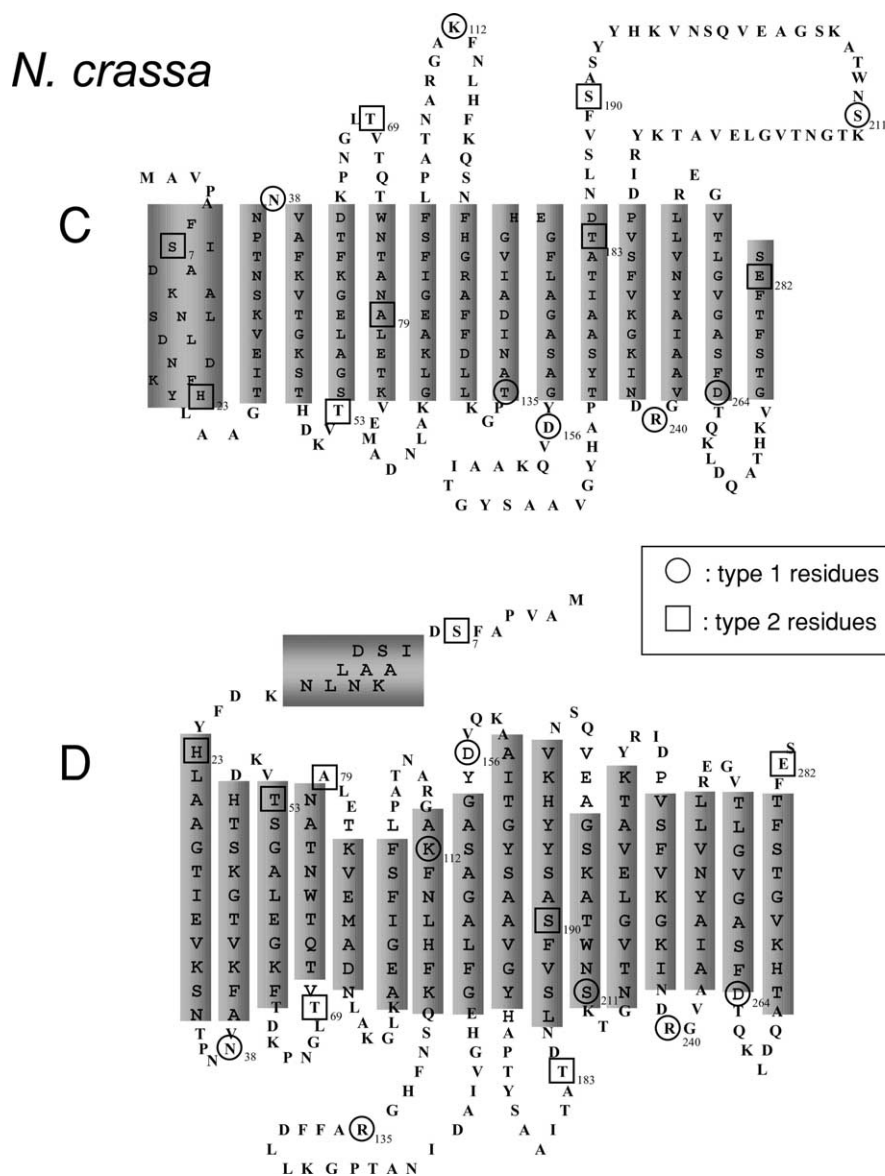
Fig. 3 (*Continued*).

experiments and modification of the native protein in its natural membrane environment.

The transmembrane topology of VDAC molecules was investigated by means of site-directed mutagenesis. Replacement of hydrophilic amino acid residues was considered to be important when it affected some electrophysiological features of the reconstituted channel. On the basis of these features, when an engineered charge change affected the channel selectivity [45] or the voltage dependence [46], the corresponding residue was proposed to be in a protein domain compatible with such a modification.

In yeast VDAC, residues involved in the channel selectivity were claimed to be inside the channel, possibly facing the aqueous interior of the pore [45]. A model with 12 β-strands and one transmembrane α-helix was designed on the basis of such mutagenesis experiments (Fig. 3A [45]). A comparison with the 3D model shows that most of the residues are in a position compatible with the experimental results (Fig. 3B). Partial exceptions are Arg124 and Gly179, which reside in the

two major loops, where they could however affect the selectivity.

The most recent model proposes that, in the open state of the pore, the single N-terminal α-helix and 13 β-strands cross the membrane forming a water-filled channel (Fig. 3C). The topology of VDAC was now probed by introducing cysteine residues into *N. crassa* VDAC, a protein otherwise devoid of cysteine residues. The engineered, purified protein was reconstituted into planar phospholipid membranes and biotinylated with a cysteine-specific reagent. Modification in the channel-forming activity of VDAC was then assayed by the addition of streptavidin, a protein with a high binding affinity for biotin [47]. Song et al. distinguished two types of residues on the basis of the effect of their modification by biotin/streptavidin. Modification of type 1 residues resulted in the reduction of single-channel conductance with no influence in the voltage dependence of the pore. Modification of type 2 residues resulted in a pore locked in a low-conducting state. In our model all type 1 residues with some slight divergence for

Lys112 are located on the surface of the channel or outside (Fig. 3D), consistent with the plug effect on the channel activity by the reported streptavidin–biotin binding [47]. Type 2 residues, with the exception of Ser190, are also present in domains located at the rim of the pore or in some extra membranous loop (Fig. 3D). Also in this case, like for the type 1 residues, these are distributed on both sides of the channel. Thus both type 1 and type 2 residues are located in areas of the model, which should be accessible to externally added bulky hydrophilic reagents.

The same authors used double mutants to determine the sidedness of single residues. We can observe that double type 2 mutants (groups 1B and 2B in [19]) fully agreed with our model. In the case of double type 2/type 1 mutants (groups 1A and 2A) the output is less clear and we noticed only partial agreements. This observation should be examined after the experimental conditions used. The voltage applied by the authors to show effects on double mutants was very high ($\pm$ 50–60 mV): this means that the pore should shift to the so-called 'closed' state. Most likely the 'closed state' implies the movement of portion(s) of the protein, thus exposing them to a bulky hydrophilic reagent. We instead assume that our model describes, statically, the 'open' state of the channel that is supposed to be different from the 'closed' state.

A different, second model consists of a pure 16 β-strand barrel. The transmembrane arrangement was validated by assessing the accessibility of single amino acid residues or stretches to proteolytic enzymes with specific cleavage sites and to specific antibodies raised against synthetic peptides corresponding to specific porin sequences [22,48]. VDAC was analysed while embedded in the mitochondrial phospholipid bilayer and not after a set of mutagenesis/expression/reconstitution. On the basis of the number of fragments generated upon proteolytic digestion the location of trypsin, chymotrypsin and V8 *S. aureus* cleavage sites was proposed in mammals [22]. These sites are located in our model in hydrophilic loops. Carboxypeptidase A digestion was not able to decrease in a significant way the size of the immunostained protein, thus suggesting no or very limited cleavage at the C-terminus of the protein [22]. The proteolytic experiments thus corroborate our present view of the transmembrane arrangement of porin.

Antisera were raised against the N-terminal end of the human and *N. crassa* VDACs. This is an excellent antigenic region [49,48]. Such antisera were always very able to detect the corresponding antigen in various situations both in Western blots and in immunostaining of fixed tissues [49,48]. It is thus most obvious that this region has to be easily accessible to a bulky hydrophilic molecule such as an IgG. Another antiserum, specific to the *N. crassa* VDAC peptide 195–210, was shown to be active against the VDAC channel in situ [48]. It recognises the sequence NSQVEA (as can be demonstrated by comparison with the corresponding yeast sequence), which is the 10/11 β-strand connecting loop, an extramembranous region, in the 3D model.

5. Conclusions

Knowledge of the secondary structure of proteins is of great interest since it may provide useful information about the properties of these molecules. In particular, designing a new model of porin, while awaiting the atomic resolution of the structure, is a necessary step for the scientists dealing with this protein. Many efforts have been made in the last 10 years to propose the most reliable and probable model for this protein [21–23,38,40,45–48]. We approached this problem with a new computational method, based on structural alignment after secondary structure prediction based on a neural network predictor suited to locate β-strands along the protein sequence.

Our neural network prediction localised 16 β-strands and one α-helix in all the eukaryotic porins tested. From this information it was deduced that VDACs could fold as a 16 β-strand barrel with a α-helix at the N-terminus, protruding outside or interacting with the membrane surface. The secondary structure prediction has been used to build a structural alignment with bacterial porins. We assumed that bacterial porins might be the best example in the nature to arrange 16 β-strands in a transmembrane barrel. A 3D model was then constructed on the basis of this structural alignment. The quality of the model is high (the percentage residues in allowed regions is comparable with that of a crystal of resolution less than 0.2 nm) in the β-barrel region but untestable in the loop regions where no obvious counterpart exists. The same is true for the N-terminal 20 residues. Its position in the model looks naive since its transmembrane location could not be predicted from bacterial structures. Our model just states that 16 β-strands have a high probability to be located in positions compatible with a β-barrel structure in VDACs.

The model is consistent with most experimental observations reported by several authors with different experimental approaches. Its most attractive feature is the assumption of large protein structures exposed on both sides of the membrane: on one side we localised large hydrophilic loops, on the other side the extra-membranous N-terminus. This disposition allows speculation about the mechanism of possible interactions between VDAC and other proteins on both sides of the mitochondrial outer membrane.

This is the first 3D model compatible with VDAC sequences. Even though it is just speculative until the molecular structure is solved or new experiments of validation are performed, it should help in designing new experiments and assigning functional features to specific parts of the protein.

The models described in the text are available as .pdb files to interested readers.

References

[1] Colombini, M. (1979) Nature 279, 643–645.
[2] Sorgato, M.C. and Moran, O. (1993) Crit. Rev. Biochem. Mol. Biol. 18, 127–171.
[3] Benz, R. (1994) Biochim. Biophys. Acta 1197, 167–196.
[4] Nikaido, H. (1994) J. Biol. Chem. 269, 3905–3908.
[5] Schulz, G.E. (1996) Curr. Opin. Struct. Biol. 6, 485–490.
[6] Weiss, M.S., Kreusch, A., Schiltz, E., Nestel, U., Welte, W., Weckesser, J. and Schulz, G.E. (1991) FEBS Lett. 280, 379–382.
[7] Cowan, S.W., Schirmer, T., Rummel, G., Steiert, M., Ghosh, R.,

Pauptit, R.A., Jansonius, J.N. and Rosenbusch, J.P. (1992) Nature 358, 727–733.

[8] Kreusch, A. and Schulz, G.E. (1994) J. Mol. Biol. 243, 891–905.

[9] Schirmer, T., Keller, T.A., Wang, Y.F. and Rosenbusch, J.P. (1995) Science 267, 512–514.

[10] Ferguson, A.D., Hofmann, E., Coulton, J.W., Diederichs, K. and Welte, W. (1998) Science 282, 2215–2220.

[11] Locher, K.P., Rees, B., Koebnik, R., Mitschler, A., Moulinier, L. and Rosenbusch, J.P. (1998) Cell 95, 771–778.

[12] Fiek, C., Benz, R., Roos, N. and Brdiczka, D. (1982) Biochim. Biophys. Acta 688, 429–440.

[13] Linden, M., Gellerfors, P. and Nelson, B.D. (1982) FEBS Lett. 141, 189–192.

[14] Crompton, M., Virji, S., Doyle, V., Johnson, N. and Ward, J.M. (1999) Biochem. Soc. Symp. 66, 167–179.

[15] Brdiczka, D. (1991) Biochim. Biophys. Acta 1071, 291–312.

[16] Krimmer, T., Rapaport, D., Ryan, M.T., Meisinger, C., Kassenbrock, C.K., Blachly-Dyson, E., Forte, M., Douglas, M.G., Neupert, W., Nargang, F.E. and Pfanner, N. (2001) J. Cell Biol. 152, 289–300.

[17] Blachly-Dyson, E. and Forte, M. (2001) IUBMB Life 52, 1–6.

[18] Dolder, M., Zeth, K., Tittmann, P., Gross, H., Welte, W. and Wallimann, T. (1999) J. Struct. Biol. 127, 64–71.

[19] Mannella, C.A., Guo, X.W. and Cognon, B. (1989) FEBS Lett. 253, 231–234.

[20] Guo, X.W. and Mannella, C.A. (1993) Biophys. J. 64, 545–549.

[21] Forte, M., Guy, H.R. and Mannella, C.A. (1987) J. Bioenerg. Biomembr. 19, 341–350.

[22] De Pinto, V., Prezioso, G., Thinnes, F., Link, T.A. and Palmieri, F. (1991) Biochemistry 30, 10191–10200.

[23] Mannella, C.A., Forte, M. and Colombini, M. (1992) J. Bioenerg. Biomembr. 24, 7–19.

[24] Rauch, G. and Moran, O. (1994) Biochem. Biophys. Res. Commun. 200, 908–915.

[25] Song, J. and Colombini, M. (1996) J. Bioenerg. Biomembr. 28, 153–161.

[26] Jacoboni, I., Martelli, P.L., Fariselli, P., De Pinto, V. and Casadio, R. (2001) Protein Sci. 10, 779–787.

[27] Kleene, R., Pfanner, N., Pfaller, R., Link, T., Sebald, W., Neupert, W. and Tropschung, M. (1987) EMBO J. 6, 2627–2633.

[28] Casadio, R., Compiani, M., Fariselli, P. and Martelli, P.L. (1999) ISBM 99 7, 68–76.

[29] Rost, B., Casadio, R., Fariselli, P. and Sander, C. (1995) Protein Sci. 4, 521–533.

[30] Vriend, G. (1990) J. Mol. Graph. 8, 52–56.

[31] Sali, A. and Blundell, T.L. (1993) J. Mol. Biol. 234, 779–815.

[32] Laskowski, R.A., MacArthur, M.W., Moss, D.S. and Thornton, J.M. (1993) J. Appl. Crystallogr. 26, 283–291.

[33] Margulis, L. (1975) Symp. Soc. Exp. Biol. 29, 21–38.

[34] Schiltz, E., Kreusch, A., Nestel, U. and Schulz, G.E. (1991) Eur. J. Biochem. 199, 587–594.

[39] Abrecht, H., Goormaghtigh, E., Ruysschaert, J.M. and Homble, F. (2000) J. Biol. Chem. 275, 40992–40999.

[35] Vogel, H. and Jahnig, F. (1986) J. Mol. Biol. 190, 191–199.

[36] Lawrence, C.E., Altschul, S.F., Boguski, M.S., Liu, S.J., Neuwald, A.F. and Wotton, J.C. (1993) Science 262, 208–214.

[37] Neuwald, A.F., Liu, J.S. and Lawrence, C.E. (1995) Protein Sci. 4, 1618–1632.

[38] Mannella, C.A., Neuwald, A.F. and Lawrence, C.E. (1996) J. Bioenerg. Biomembr. 28, 163–169.

[40] Guo, X.W., Smith, P.R., Cognon, B., D'Arcangelis, D., Dolginova, E. and Mannella, C.A. (1995) J. Struct. Biol. 114, 41–59.

[41] Colombini, M., Yeung, C.L., Tung, J. and König, T. (1987) Biochim. Biophys. Acta 905, 277–286.

[42] Benz, R., Kottke, M. and Brdzicka, D. (1990) Biochim. Biophys. Acta 1022, 311–318.

[43] Bainbridge, G., Gokce, I. and Lakey, J.H. (1998) FEBS Lett. 431, 305–308.

[44] Holden, M.J. and Colombini, M. (1993) Biochim. Biophys. Acta 1144, 396–402.

[45] Blachly-Dyson, E., Peng, S.Z., Colombini, M. and Forte, M. (1990) Science 247, 1233–1236.

[46] Thomas, L., Blachly-Dyson, E., Colombini, M. and Forte, M. (1993) Proc. Natl. Acad. Sci. USA 90, 5446–5449.

[47] Song, J., Midson, C., Blachly-Dyson, E., Forte, M. and Colombini, M. (1998) J. Biol. Chem. 273, 24406–24413.

[48] Stanley, S., Dias, J.A., D'Arcangelis, D. and Mannella, C. (1995) J. Biol. Chem. 270, 16694–16700.

[49] Babel, D., Walter, G., Götz, H., Thinnes, F.P., Jürgens, L., König, U. and Hilschmann, N. (1991) Biol. Chem. Hoppe-Seyler 372, 1027–1034.